

# Effect of Common U.S. Ground Motion Selection Methods on the Structural Response of Steel Moment Frame Buildings

Raul Uribe,<sup>a)</sup> Siamak Sattar,<sup>b)</sup> M.EERI, Matthew S. Speicher,<sup>b)</sup> and Luis Ibarra<sup>a)</sup>

This study quantifies the impact of two common ground motion (GM) selection methods, included in U.S. standards, on the seismic performance evaluation of steel special moment frames. The methods investigated are a “traditional” approach, herein referred to as the target maximum considered earthquake (TMCE) method, and a newer approach known as the conditional mean spectrum (CMS) method. The TMCE method selects GMs using the risk-based maximum considered earthquake ( $MCE_R$ ) spectrum as the target spectrum, while the CMS method uses the CMS that anchors the  $MCE_R$  at multiple conditioning periods. Three special steel moment frames of 4, 8, and 16 stories are designed in accordance with ASCE/SEI 7-10, and their seismic performance is assessed with the nonlinear dynamic procedure prescribed in ASCE/SEI 41-13 using GMs selected and scaled in accordance with the aforementioned methods. A comparison of statistical parameters for the reduced beam sections and column hinges is conducted using the normalized demand-to-capacity ratio ( $DCR$ ), as the output parameter. The buildings are evaluated at the collapse prevention performance level for a far-field site located in Los Angeles, CA. In general, the CMS method results in lower  $DCRs$  of the frame components and smaller output parameter dispersion. In addition to the spectral shape, the demands are largely influenced by the spectral accelerations prescribed for each evaluated method. The consideration of collapse realizations is also documented as well as the existing and proposed statistical methods to account for these realizations. The study shows that the GM selection process can cause significant differences in structural response that may lead to different retrofitting decisions. [DOI: 10.1193/122917EQS268M]

## INTRODUCTION

One of the main steps in the assessment of nonlinear dynamic response of buildings is the selection of an appropriate suite of ground motions (GMs). The available GM selection methods vary in terms of the selection criteria, error computation, and target spectrum, among other factors. The common premise of these methods is to select records that reasonably estimate GMs anticipated to occur in a future earthquake at a specific site. In general, GM selection and scaling methods can be categorized as (1) amplitude scaling or (2) spectral

---

<sup>a)</sup> University of Utah, 110 Central Campus Drive, Salt Lake City, UT 84112; Email: raul.uribe@utah.edu (R. U.)

<sup>b)</sup> National Institute of Standards and Technology, 100 Bureau Drive, MS 8604, Gaithersburg, MD 20899

matching (i.e., modification of frequency content). [Haselton et al. \(2009\)](#) summarizes various approaches to select and scale GMs.

This study focuses on two GM selection methods that are currently recommended in U.S. codes and standards: (1) a target design spectrum approach, denoted in this study as the target maximum considered earthquake (TMCE), which is a well-established method used in research and practice, and (2) the conditional mean spectrum (CMS) method, a newer method that has been employed more in research. In the TMCE method, GMs are selected to minimize the error between each GM spectrum and the target spectrum (risk-based maximum considered earthquake ( $MCE_R$ ) in this study) across a range of periods. The approach is implemented in the PEER online tool. Other studies have used methods similar to the TMCE method that match records to the  $MCE_R$  spectrum while minimizing the error in a specified range for use in nonlinear analyses (e.g., [Kalkan and Chopra 2010](#)). In contrast, the CMS method uses the CMS as the target spectrum for scaling GMs to match the spectral acceleration ( $S_a$ ) at a conditioning period ([Baker 2011](#), [Uribe et al. 2017](#)). For the simplest case in which only one conditioning period is used, the CMS method produces a record set with no dispersion at this period, and it can be considered a single target spectral acceleration approach ([Adam et al. 2017](#)). There are other methods in which GMs are selected to match both the standard deviation,  $\sigma_{lnSa}(T_i)$ , and mean of the GM spectra computed from a GM prediction model (GMPM), such as the conditional spectra (CS) method (e.g., [Lin et al. 2013](#)) and the generalized conditional intensity measure method ([Bradley 2010](#)). Recent studies have modified the CS method by changing the conditioning intensity measure to the average spectral acceleration ([Kohrangi et al. 2017](#)), which enhances the efficiency in estimating several engineering demand parameters simultaneously, but these methods are not currently included in American standards and are not part of this study. To investigate the effect of these GM selection methods on the system's response, ASCE/SEI 7-10–designed 4, 8, and 16-story buildings are analyzed using the nonlinear dynamic procedure outlined in ASCE/SEI 41-13 ([American Society of Civil Engineers \(ASCE\) 2014](#)), hereafter referred to as ASCE 41. The predicted performance of the buildings, in terms of nonlinear hinge deformations and their corresponding dispersion, is compared for the CMS and TMCE GM selection methods. The selected GM level leads to collapse realizations that need to be considered in the seismic performance evaluation. The study also shows the limitations of current guidelines to account for these realizations.

## BACKGROUND ON GM SELECTION AND SCALING METHODS

### CMS METHOD BACKGROUND

In this site-specific GM selection method, the scaled records are chosen based on how closely they match a conditional mean target spectrum across a range of vibrational periods ([Baker 2011](#)). The CMS is a more realistic target for selecting and scaling GMs because the alternative uniform hazard spectrum conservatively assumes that all the high spectral accelerations associated with the target hazard level occur in a single event ([Baker 2011](#)). Instead, the CMS is conditioned, or anchored, to a single spectral acceleration at a period of significance, such as the building's fundamental period. In this study, the risk-targeted  $MCE_R$  is selected as the spectrum to anchor the CMS, and it is computed following ASCE/SEI 7 ([ASCE 2010](#)) recommendations. Once the spectral acceleration at the conditioning period,  $T^*$  (i.e., the period in which the spectral acceleration of the CMS matches the  $MCE_R$ ) is determined, the median GM spectrum is calculated using the Campbell and Bozorgnia GMPM ([Campbell and Bozorgnia 2008](#)). The mean CMS spectrum,  $\mu_{lnSa(T_i)|lnSa(T^*)}$ , is computed as follows:

$$\mu_{\ln Sa(T_i)|\ln Sa(T^*)} = \mu_{\ln Sa}(M, R, T_i) + \rho(T_i, T^*)\varepsilon(T^*)\sigma_{\ln Sa}(T_i) \quad (1)$$

where  $\mu_{\ln Sa(T_i)|\ln Sa(T^*)}$  is the logarithmic mean  $S_a$  at period  $T_i$  for a spectrum anchored at conditioning period  $T^*$ , and  $\mu_{\ln Sa}(M, R, T_i)$  is the median GM, also denoted as the logarithmic mean of  $S_a$ . The parameters  $M$  and  $R$  are the earthquake mean magnitude and mean distance from deaggregation,  $\rho(T_i, T^*)$  is the correlation coefficient between  $\varepsilon$  at  $T_i$  and  $T^*$ ,  $\varepsilon(T^*)$  represents the number of standard deviations the target spectral acceleration differs from the median GM at the conditioning period (Baker 2011), and  $\sigma_{\ln Sa}(T_i)$  is the logarithmic standard deviation of  $S_a$  from the GMPM (Lin et al. 2013). In Figure 1, the CMS has lower spectral accelerations than the  $MCE_R$  spectrum, with the exception of the acceleration at the conditioning period ( $T^* = T_1$ ), which matches the  $MCE_R$ . Note that this conditioning period  $T^*$  can also be “anchored” to other vibrational periods in the  $MCE_R$  spectrum.

The GMs are selected based on how similar their response spectra are compared with the CMS. The GMs with the smallest sum of squared errors (SSE; Baker 2011) in the period interval of interest (from  $0.2T_1$  to  $2T_1$  in this study) are selected.

## TMCE METHOD BACKGROUND

This method scales GMs to minimize the error between each GM spectrum and the target spectrum,  $MCE_R$ , across a range of periods. The difference between the target spectrum and individual spectra is computed using the mean squared error (MSE):

$$MSE = \frac{\sum_i w(T_i) \{ \ln[S_a^{target}(T_i)] - \ln[f * S_a^{record}(T_i)] \}^2}{\sum_i w(T_i)} \quad (2)$$

where  $w(T_i)$  is the weight assigned to the period  $T_i$ ,  $S_a^{target}$  is the target spectral acceleration,  $S_a^{record}$  is the individual record spectral acceleration, and  $f$  is the linear scale factor assigned to the GM. In this study,  $w$  is set to 1.0 across the period range of interest. By setting  $w = 1.0$ ,

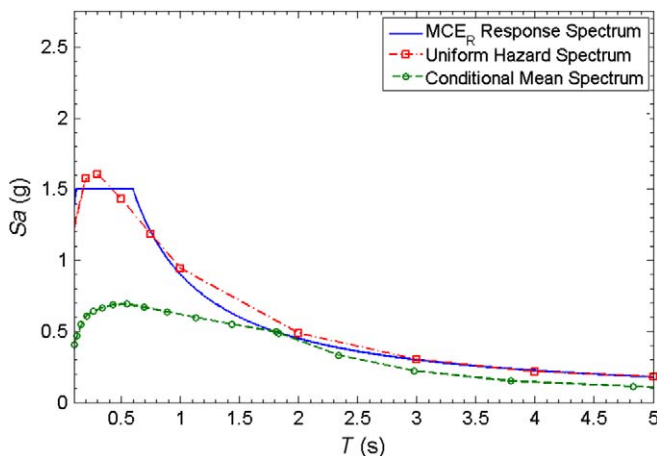


**Figure 1.** Comparison of the uniform hazard spectrum,  $MCE_R$  spectrum, and CMS conditioned at  $T^* = T_1 = 1.81$  s for the 4-story frame of this study.

the MSE computation is reduced to the SSE method. The factor  $f$  is automatically optimized to have the smallest MSE achievable within the same range of periods as the weight function.

## BUILDING DESCRIPTION AND MODELING

### BUILDING DESCRIPTION

The 4, 8, and 16-story buildings are designed in accordance with the International Building Code (International Code Council 2012) and its referenced standards ASCE/SEI 7 (ASCE 2010) and AISC 341-10 (American Institute of Steel Construction 2010). The seismic force-resisting system is an exterior three-bay special moment frame (SMF) in the east-west direction and an exterior two-bay special concentrically braced frame in the north-south direction. This study focuses only on the SMF performance, in which the 4, 8, and 16-story frames have fundamental periods of vibration of 1.81, 2.79, and 4.12 s, respectively. Figure 2a and 2b shows a typical building floor plan and SMF elevations for the 4 and 8-story buildings, respectively. Reduced beam sections (RBSs) are used for beam-to-column connections, and columns are sized to satisfy strong-column/weak-beam requirements. Additionally, columns are upsized where necessary to avoid the use of double plates to strengthen the column webs, to reflect common design practice. The buildings are assumed to be located on a site with stiff soil (Site Class D) and assigned to Seismic Design Category D with spectral accelerations

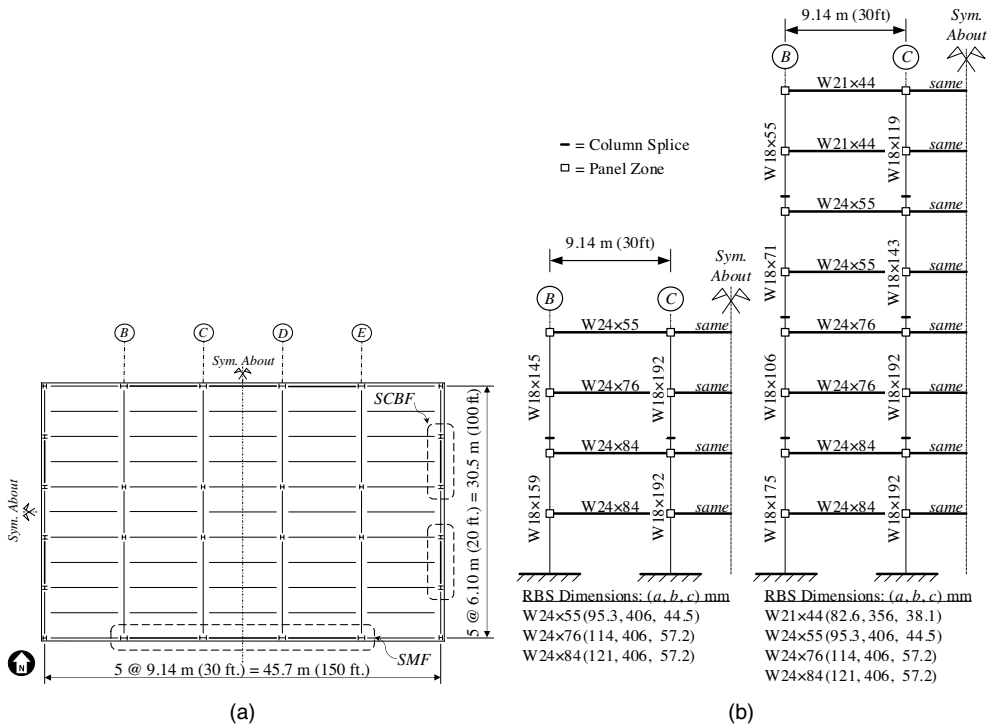


**Figure 2.** Archetype buildings: (a) floor plan; (b) SMF elevations of 4 and 8-story frames.

$S_S = 1.5 \text{ g}$  at  $T_s = 0.2 \text{ s}$  and  $S_1 = 0.59 \text{ g}$  at  $T_1 = 1.0 \text{ s}$ . Detailed information regarding building description and design process can be found in Harris and Speicher (2015).

## BUILDING MODELING

The three-dimensional buildings are modeled in PERFORM-3D (Computers and Structures, Inc. 2011). The gravity frames include elastic beams and columns and pinned beam-to-column connections. The beam nonlinear behavior is modeled with moment-curvature hinges placed at the centerline of each RBS. The RBS reduced stiffness is captured by a prismatic section over the entire length of the RBS with a moment of inertia equal to that of the section at one-third from the center of the RBS. The nonlinear behavior of the columns is modeled with moment-curvature hinges that account for axial-moment interaction (i.e., PMM hinge element in PERFORM-3D). These column hinges are placed at a distance  $d_c/2$  from the face of the beam, where  $d_c$  is the column depth. The 1st story column base is modeled as a fixed boundary condition. Lastly, the nonlinear behavior in the panel zones is modeled with PERFORM-3D's panel zone element (Krawinkler 1978). These nonlinear component models are initially constructed using modeling parameters defined in ASCE/SEI 41 table 9-6 and then qualitatively calibrated against experimental tests (Harris and Speicher 2015).

The nonlinear time history analysis may terminate earlier when the solution fails to converge or when an arbitrary roof drift ratio of 20% is reached. Collapse modes not modeled herein (e.g., failures in the gravity framing system) would likely occur well before 20% is reached. The impact of modeling uncertainty (Sattar et al. 2013, Ibarra and Krawinkler 2005a) is not considered in this study.

## OUTPUT PARAMETER

The maximum interstory drift ratio is usually adopted as the global structural response parameter for moment-resisting frames because it is an effective global representation of local joint rotations (Miano et al. 2017) that correlates to structural damage (Krawinkler et al. 2004). Therefore, the frame performance is presented in terms of demand-to-capacity ratio (DCR), computed as follows (Harris and Speicher 2015):

$$\text{Deformation-controlled action: } DCR = \frac{\theta_{total}}{\kappa(\theta_y + \theta_{pe} + \theta_{p,AC})} \quad (3)$$

$$\text{Force-controlled action: } DCR = \frac{\theta_{total}}{\kappa\theta_y} \quad (4)$$

where  $\theta_y$  is the yield deformation,  $\theta_{pe}$  is the post-yield elastic deformation,  $\theta_{total}$  is the total deformation,  $\theta_{p,AC}$  is the acceptance criterion range based on plastic deformation defined in ASCE/SEI 41 (Figure 3). The knowledge factor,  $\kappa$ , is taken as unity since information for new buildings is known. The total deformation is used because PERFORM-3D moment-curvature output is expressed in terms of total curvature (moment-curvature hinges are used for the columns and beams). The acceptance criteria for all elements are set to the collapse prevention performance level for the three buildings. Beam-to-column connections and panel zone rotation are generally considered to be deformation controlled, while the column rotation

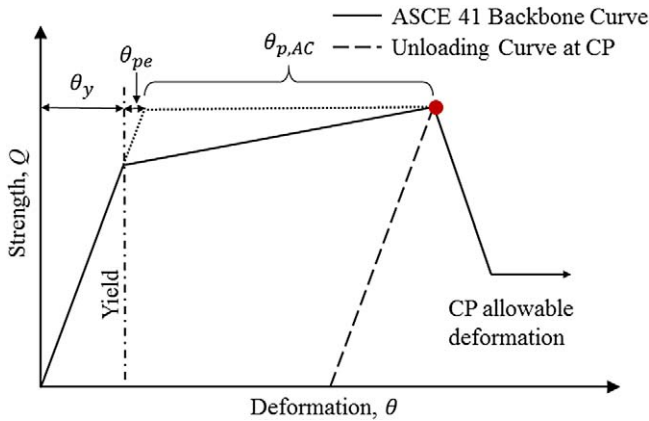


**Figure 3.** Generalized component backbone curve.

classification depends on the level of axial load. For the frame columns, the axial load must reach at least 50% of its axial capacity for the component to be considered a force-controlled action.

### IMPLEMENTATION OF GM SELECTION

The buildings are considered to be located in Los Angeles, CA, and a far-field site within the city area is selected based on the soil classification and mean rupture distance. The selected soil type matches the site class used in the archetype building design, i.e., the National Earthquake Hazards Reduction Program, soil type D with an average shear wave velocity ( $V_{s30}$ ) of 180–360 m/s (U.S. Geological Survey (USGS) 2016). The selected site has a  $V_{s30}$  value of 300–360 m/s. The site is selected to satisfy the ASCE/SEI 7-16 requirements for a far-field site located more than 15 km from a rupture plane. A site can also be considered far-field in the 10–15 km range as long as the magnitude of the earthquake is less than  $M_w = 7.0$  (ASCE 2016). In this study, the rupture distance is between 10 and 110 km. The selected far-field site (latitude/longitude = 34.197/–118.645) has a mean rupture distance of 17.2 km, according to the deaggregation computed with the USGS tool.

The criteria for the selection and scaling of GMs meet or exceed ASCE/SEI 7 requirements for the two investigated methods and are as follows:

1. Fourteen GM records are selected. The number of records is consistent with a previous study (Harris and Speicher 2015), and it is larger than the 11 records required by ASCE/SEI 7-16. Note that 14 records are usually at the lower bound of the number of records that provide statistical meaningful results (e.g., Jalayer 2003).
2. The scale factor on individual records is no greater than 2.5 (ASCE/SEI 7-16 limits the scale factor to 4.0).
3. No more than one record is selected from the same recording station.
4. No more than three records are selected from the same event.

ASCE/SEI 7-16 (ASCE 2016) is used for the GM selection because it is the first standard that includes recommendations for the CMS method. The scale factor cap of 2.5 keeps the GM characteristics and shape closer to what may be expected based on the recorded motions. The limitations on the amount of records included in the GM suite from a certain recording station or event prevent the suite from being overly influenced by a single event.

## CMS METHOD IMPLEMENTATION

The main CMS conditioning period is the fundamental period of the system,  $T_1$ . Additional conditioning periods are selected to (1) account for different structural performance aspects (National Institute of Standards and Technology 2011) and (2) satisfy the ASCE/SEI 7-16 requirement of having the envelope of the target spectra exceed 75% of the  $MCE_R$  between the period interval of interest. A short conditioning period is used to account for higher mode contributions, while a long period accounts for period elongation effects (Lin et al. 2013). This study uses a lower limit of  $0.2T_1$  and an upper limit of  $2T_1$  for the bounds of the period range, as recommended by ASCE/SEI 7-16. Then periods of  $0.2T_1, T_1$ , and  $2T_1$  are initially selected as the conditioning periods. A fourth conditioning period of  $0.4T_1$  is added in the 4 and 8-story buildings to ensure the envelope spectrum exceeds 75% of the  $MCE_R$  between  $0.2T_1$  and  $2T_1$ . The CMS conditioning period that leads to the largest median  $DCR$  is referred to as the controlling CMS period.

For each conditioning period, GMs are selected following the procedure developed by Jayaram et al. (2011), and the tool developed by Baker (2016) is used to automate the GM selection process. Figure 4a shows the 14 GMs selected using the CMS method for the 4-story building conditioned at the fundamental period,  $T_1$ . Figure 4b presents the target and average mean spectra for the selected four conditioning periods (i.e.,  $0.2T_1, 0.4T_1, T_1$ , and  $2T_1$ ).

## TMCE METHOD IMPLEMENTATION

The PEER NGA-West2 database tool (PEER 2016) is used to select GMs based on minimizing the error (MSE) across the period range of  $0.2T_1$  and  $2T_1$  with respect to the  $MCE_R$  target spectrum. The tool input parameters include magnitude, rupture distance, shear wave velocity, scale factor, weight function, and fault type (although only the strike-slip fault type is considered).

The selected GMs, which were already individually scaled to minimize the MSE (with a scaled factor no greater than 2.5), are scaled for a second time using a single scale factor applied to all records in the set to ensure that the spectral GM arithmetic mean (average) does not drop below the target spectrum between  $0.2T_1$  and  $2T_1$  (ASCE/SEI 7-16). The total scale factor after these two steps is still less than 4.0. Figure 4c shows the average of 14 GMs selected using the TMCE method for the 4-story building. A comparison of Figure 4a and 4c shows that the TMCE method minimizes  $S_a$  dispersion over a period interval of interest, whereas the CMS method is a target  $S_a$  approach that produces a record set with null dispersion at the conditioning period, dispersion that rapidly increases as the period changes. However, the CMS method is usually implemented with several conditioning periods, as in this study, and there are as many target  $S_a$  as conditioning periods.

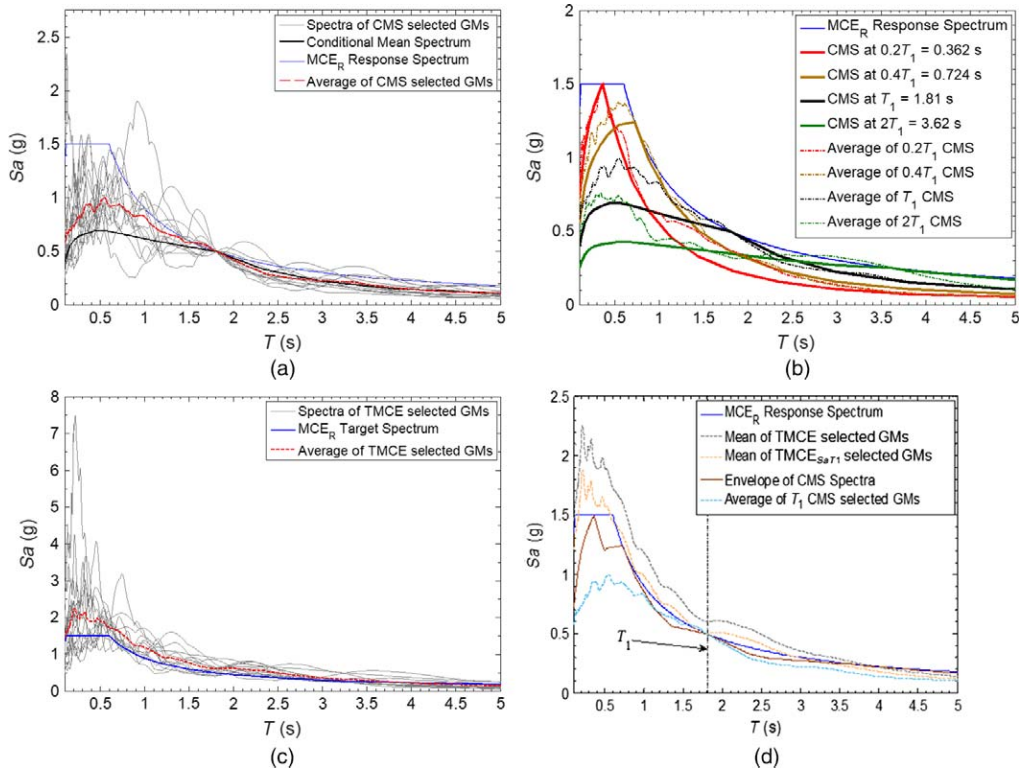


**Figure 4.** Spectra for 4-story building: (a) response spectra of GMs for CMS method conditioned at  $T_1 = 1.81$  s, (b) target and average CMS spectra for four conditioning periods, (c) response spectra of GMs using the TMCE method, and (d) comparison of TMCE,  $TMCE_{SaT_1}$ , and CMS spectra.

Figure 4d shows that the mean TMCE spectrum accelerations are higher than those of the mean CMS envelope between  $0.2T_1$  and  $2T_1$  for the 4-story frame. This observation is consistent for all the frames because the mean TMCE spectrum accelerations are required to be larger than  $MCE_R$  spectrum accelerations in the period interval of interest, whereas the mean CMS envelope accelerations only need to meet the 75% spectral acceleration criterion. These different code requirements affect the comparison of GM selection methods because the TMCE method leads to larger inelastic building responses than CMS records, not only because of the spectrum shape but also because of these larger accelerations. To evaluate the effect of the spectral shape in the GM selection approach, a variation of the TMCE method is investigated, in which the average (mean) spectrum of the 14 TMCE records is scaled down to match the spectral acceleration of the  $MCE_R$  spectrum at  $T_1$  and is denoted as  $TMCE_{SaT_1}$  or TMCE at  $S_a(T_1)$  (see Figure 4d). The scaled-down TMCE spectral accelerations are lower by approximately 20%, 70%, and 95% for the 4, 8, and 16 stories, respectively, from the original TMCE spectra. Figure 4d also shows the envelope CMS spectrum and the average of the  $T_1$  CMS

spectrum. A comparison of average CMS and  $TMCE_{SaT_1}$  spectra shows that, if  $T_1$  is the controlling period, the spectral accelerations around the fundamental period are similar, but CMS accelerations can be less than half the TMCE spectral accelerations for shorter and longer conditioning periods. However, the envelope of the CMS spectra curve, which is ultimately used for the analyses, exhibits larger accelerations, especially in the short period range. For the 4 story (Figure 4d) and 16-story frames, the envelope of CMS spectra curve has smaller accelerations than those of the  $TMCE_{SaT_1}$  spectra. But for the 8-story frame, not shown, the accelerations of the envelope of CMS spectra in the short period range are larger than those of the  $TMCE_{SaT_1}$  spectra. This counterintuitive outcome is caused by (1) the TMCE reduction to match  $S_a$  at  $T_1$  (i.e., to generate  $TMCE_{SaT_1}$  spectra) and (2) the use of an envelope CMS spectrum to ensure that CMS accelerations are at least 75% of  $MCE_R$  spectrum accelerations.

### DCR RESULTS

Nonlinear dynamic analyses were carried out to obtain the individual *DCR* of the frame components, using the CMS and TMCE methods for selecting the GMs. A maximum roof drift limit (RDL) of 20% was arbitrarily selected to terminate the analysis in cases where collapse occurred or the solution algorithm failed to converge. The threshold of 20% was chosen because it is unlikely that collapse drifts will exceed this limit. Table 1 shows that CMS and TMCE methods lead to different numbers of realizations reaching the 20% RDL. As can be seen, the original TMCE method leads to more collapses than the CMS and  $TMCE_{SaT_1}$  methods. Table 1 also shows the controlling CMS period for the collapsed cases, which have controlling periods  $T^* = 0.4T_1$  and  $T^* = T_1$  for the 4 and 8-story frames, respectively. The 16th story frame did not exhibit collapsed realizations under the CMS method.

To compare the output parameters obtained from the studied GM selection methods, the *DCR* data were processed following two statistical approaches. First, a lognormal

**Table 1.** Total collapse cases caused by CMS and TMCE-selected GMs

Building	GM selection method	No. of GMs that lead to collapse	Controlling CMS period for collapse realizations
4 story	CMS	1	$0.4T_1$
	Original TMCE	2	N/A <sup>a</sup>
	$TMCE_{SaT_1}$	1	N/A
8 story	CMS	1	$T_1$
	Original TMCE	4	N/A
	$TMCE_{SaT_1}$	1	N/A
16 story	CMS	0	N/C <sup>b</sup>
	Original TMCE	2 <sup>c</sup>	N/A
	$TMCE_{SaT_1}$	0	N/A

<sup>a</sup> N/A: Controlling CMS period not applicable.

<sup>b</sup> N/C: No collapse detected under CMS method.

<sup>c</sup> One collapse and a realization with no convergence (treated as a collapse).

probability density function was assumed to address the inherent inconsistencies of collapsed cases. In this case, the median was computed as the 50th point of the sorted data. Second, the average or arithmetic mean was computed, as recommended in ASCE/SEI 41 (ASCE 2014).

### **DCR STATISTICAL RESULTS BASED ON A LOGARITHMIC SORTED DATA APPROACH**

This sorted data approach assumes that the evaluated data reasonably fit a lognormal distribution. A series of Kolmogorov-Smirnov tests on the *DCR* data demonstrated that the lognormal distribution fits a majority of the *DCR* data more appropriately than a normal distribution (Uribe et al. 2018). This is an expected result given that the data have only positive values and the distribution is skewed to the right (Shome and Cornell 1999). By assuming a lognormal distribution, the mean can be computed from the sorted median  $x_{50}$  as follows:

$$\mu_x = x_{50} \cdot e^{\frac{\sigma_{lnx}^2}{2}} \quad (5)$$

where  $\sigma_{lnx}$  is the standard deviation of the natural logarithm of *DCR* values and is calculated as (Ibarra and Krawinkler 2005b):

$$\sigma_{lnx} = \ln \left( \sqrt{\frac{x_{84}}{x_{16}}} \right) \quad (6)$$

where  $x_{16}$  and  $x_{84}$  are the 16th and 84th percentiles of the *DCR* values for each element. Note that  $\sigma_{lnx}$  and  $\mu$  are computed in such a way that the collapse of a couple of realizations does not force the use of the arbitrary RDLs. Because this study uses 14 GMS, the 84th percentile can be computed with the lowest 12 drifts, and the calculations are not affected by one or two collapsed frames. If more than two realizations lead to collapse,  $\sigma_{lnx}$  could be estimated based on the 16th and 50th (Ibarra and Krawinkler 2005b), as long as the noncollapsed frames are sufficient to obtain the median value. However, this approach is not considered for two reasons. First, the use of the 16th and 84th percentiles is expected to provide more consistent results, since the probabilistic distribution interval spans two standard deviations. More importantly, drifts of noncollapsed cases below the 50th may be relatively small for most realizations, which may result in realizations in which the mean *DCR* (or any selected percentile) is less than unity, even if a large number of collapses occur.

Thus two building performance acceptance criteria are proposed for the sorted data approach:

1.  $DCR < 1.0$ , whether the parameter is based on the mean or a given percentile, such as the 84th. In the following results, this criterion is based on mean curves.
2. The collapsed cases have to be less than 16% of the realizations. Therefore, the 84th percentile in Equation 6 will not include data from collapse realizations.

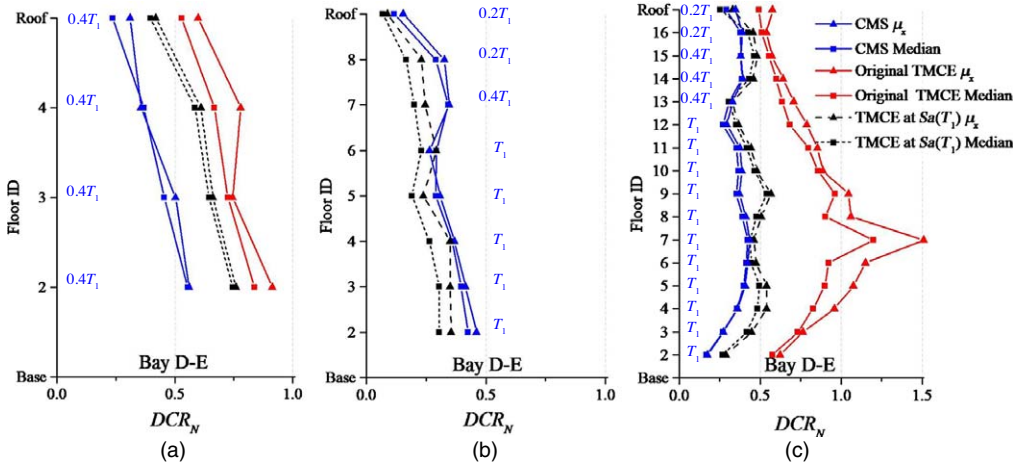
## RESULTS FOR MEANS AND MEDIANS FOR *DCR* BASED ON A SORTED DATA APPROACH

Figure 5a–5c plots the mean and median response in terms of *DCR* for the beams using a lognormal distribution for the 4, 8, and 16-story buildings, respectively. The means and medians are similar when no collapses are included in Equations 5 and 6. The plots compare mean *DCR*s when using the CMS ( $\mu_{DCR,CMS}$ ), original TMCE ( $\mu_{DCR,TMCE}$ ), and  $TMCE_{SaT1}$  ( $\mu_{DCR,TMCE,T1}$ ) GMs. The *DCR* values for the CMS method correspond to those of the controlling CMS period that produces the largest mean *DCR*s ( $\mu_{DCR,CMS}$ ) at each floor. In the case of the 4-story building, for instance, the controlling period for all the RBS elements is  $0.4T_1$ . In this building, the CMS method provides lower mean *DCR*s than those of the original TMCE method at every floor. These differences result in  $\mu_{DCR,CMS}/\mu_{DCR,TMCE}$  ratios as low as 0.46, based on the comparison of drifts at each floor. The 4-story frame passes the sorted data acceptance criteria for the CMS and original TMCE methods because the number of collapses (one case) is less than 16%, and the mean *DCR* are less than unity; see Figure 5a.

The 8-story frame curves are not reported for the original TMCE method because this case exhibited four collapses (Table 1), exceeding 16% of the realizations. Thus this building does not meet the second sorted data acceptance criterion under the original TMCE method, and it should be redesigned or retrofitted. The CMS method, however, still produces  $\mu_{DCR,CMS}$  values for this frame lower than unity, as observed in Figure 5b. For the 16-story frame, the CMS method also leads to  $DCR < 1.0$ . The TMCE method can be computed because only two realizations were not completed (Table 1), but the  $\mu_{DCR,TDS}$  are larger than 1.0 in several floors, and the performance is not acceptable under this GM selection method. Note that the  $\mu_{DCR,CMS}/\mu_{DCR,TMCE}$  ratios can be as low as 0.28.

The original  $\mu_{DCR,TDS}$  values are larger than those obtained from the CMS method, not only because of the mean spectral shapes, but also because  $S_a(T_1)$  is larger for the TMCE method (Figure 4d). To isolate the spectral shape effect, the TMCE spectrum is scaled down to match the  $MCE_R S_a(T_1)$ . Figure 5a–5c also presents the beam *DCR* means and medians obtained from the  $TMCE_{SaT1}$  ( $\mu_{DCR,TMCE,T1}$ ) spectrum. The *DCR* curves can be computed for the three evaluated frames, given that no more than one collapse is reported in each case (Table 1). Although the mean CMS and  $TMCE_{SaT1}$  curves are closer to each other, the CMS still results in smaller drifts for the 4 and 16-story frames, with  $\mu_{DCR,CMS}/\mu_{DCR,TMCE,SaT1}$  ratios as low as 0.58 and 0.60, respectively. For the 8-story frame, the CMS method results in larger drifts (i.e.,  $\mu_{DCR,CMS}/\mu_{DCR,TMCE,SaT1} > 1$ ) for all stories, except the 6th floor. The likely reason is that the CMS spectrum for the 8-story frame has higher spectral accelerations in the short period range, unlike the 4 story (Figure 4d) and 16-story frames.

Figure 6 presents mean *DCR* curves at column hinges for the 4, 8, and 16-story frames obtained from the sorted data approach. In the 4 and 16-story frame columns, the CMS method leads to the lowest drifts or *DCR*, with  $\mu_{DCR,CMS}/\mu_{DCR,TMCE}$  ratios as low as 0.34 and 0.15, respectively. However, when the TMCE spectrum is scaled down, the *DCR*s are closer to those obtained by the CMS method. For example, the smallest  $\mu_{DCR,CMS}/\mu_{DCR,TMCE,SaT1}$  ratio in the 4-story frame is 0.41. In the 16-story frame, the  $\mu_{DCR,CMS}/\mu_{DCR,TMCE,SaT1}$  ratios are as low as 0.57 with three upper floor ratios exceeding



**Figure 5.** Sorted data approach: mean and median of  $DCR$  for RBSs, using the CMS and TMCE and  $TMCE_{Sa(T_1)}$  GM selection methods for the (a) 4-story, (b) 8-story, and (c) 16-story frames (the  $DCR$  values for the CMS method correspond to those of the controlling period).

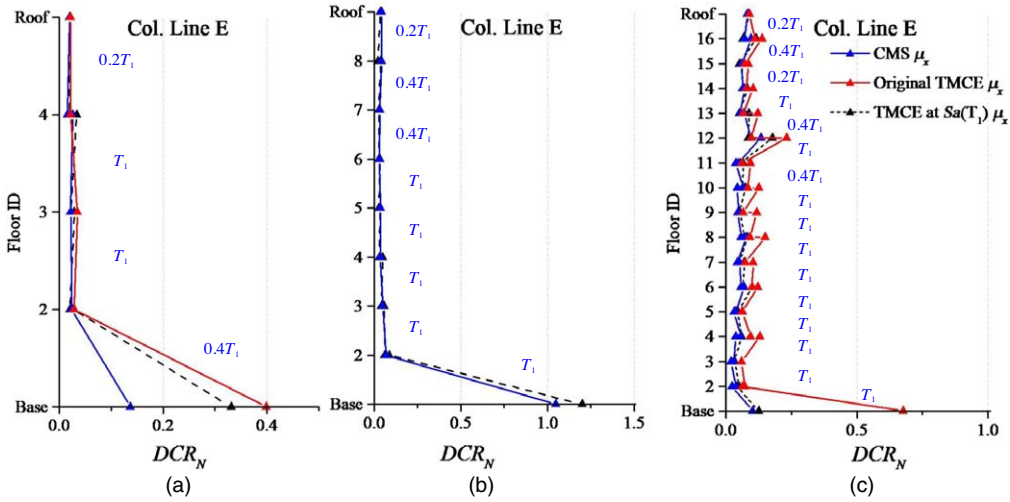


**Figure 6.** Sorted data approach: mean curves of maximum  $DCR$  for column hinges using the CMS and TMCE and  $TMCE_{Sa(T_1)}$  GM selection methods for the (a) 4-story, (b) 8-story, and (c) 16-story frames (the  $DCR$  values for the CMS method correspond to those of the controlling period).

unity, which indicates that the CMS  $DCR$ s are larger than those of  $TMCE_{SaT_1}$ . The  $DCR$ s for the columns of the 8-story frame obtained from the CMS and  $TMCE_{SaT_1}$  methods are very similar. Note that Figure 6b does not show 8-story frame  $DCR$ s for the TMCE method because the number of collapses exceeded 16% of the realizations.

## UNCERTAINTY IN RESPONSE PREDICTION FOR *DCR* BASED ON THE SORTED DATA APPROACH

One of the primary goals of efficient GM selection methods is to carry out a meaningful evaluation of the structural seismic response with the smallest possible number of records. In this context, the efficiency of the GM set increases if the variability in the response parameters decreases. Some authors also consider that GM efficiency should lead to lower scaling factors (e.g., Miano et al. 2017). To determine the uncertainty associated with the results produced by each GM selection approach, the *DCR* standard deviation is computed for each element using Equation 6. These dispersions are not intended to be used to evaluate the accuracy of the evaluated GM selection methods, but to compare the two methods relative to each other and indicate the number of records that may be needed to accurately compute the mean or median response.

Figures 7–9 show the standard deviation in the *DCR*s obtained from different GM selection methods for the 4, 8, and 16-story frames, respectively. In the 4-story frame, the dispersion in the beams does not show a defined trend for the CMS method. Moreover, the standard deviation values obtained from the TMCE and  $TMCE_{SaT_1}$  methods ( $\sigma_{DCR, TMCE}$  and  $\sigma_{DCR, TMCE, SaT_1}$ ) are smaller, except on the fourth floor. As for the column hinges (Figure 7b), the CMS method provides a lower dispersion ( $\sigma_{DCR, CMS}$ ) for the 2nd and 3rd story. For the 8 and 16-story frames the dispersion is lower for most of the beams and columns when applying the CMS method (Figures 8 and 9). The CMS method usually renders a lower dispersion than the original TMCE method, partially because of its lower spectral accelerations, but there are other factors involved.

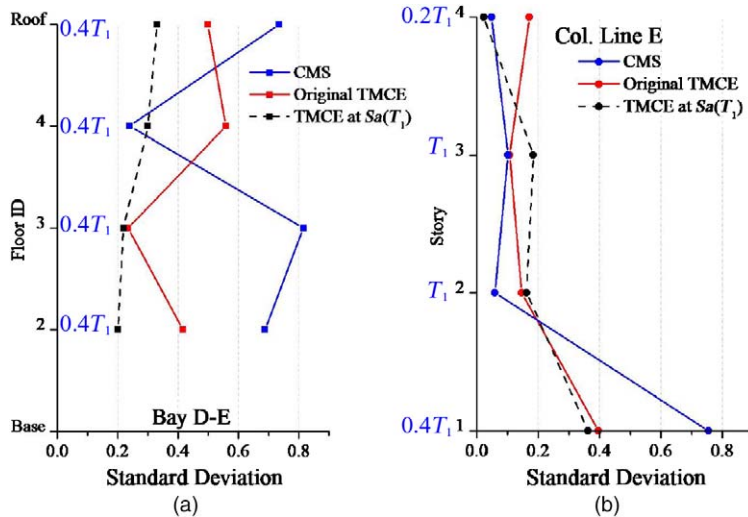


**Figure 7.** Standard deviation of the *DCR* results for the 4-story building of the (a) RBS connections in bay D-E and (b) column hinges in the column located on column line E using CMS at the controlling period and TMCE methods.

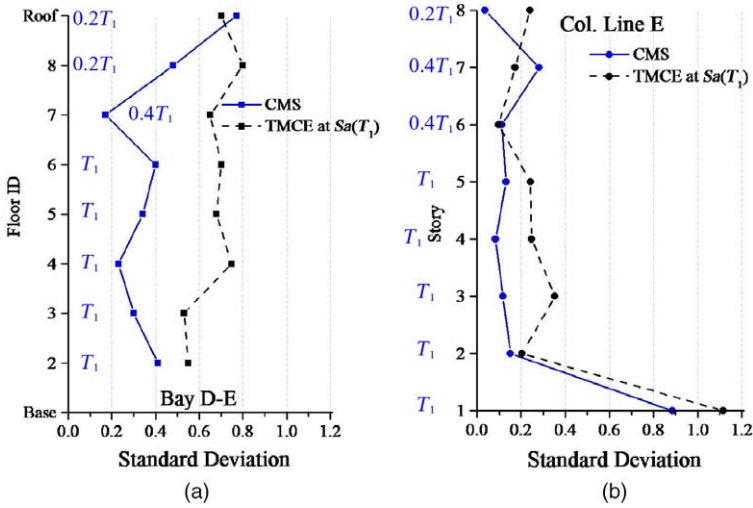


**Figure 8.** Standard deviation of the *DCR* results for the 8-story building of the (a) RBS connections in bay D-E and (b) column hinges in the column located on column line E using CMS at the controlling period and TMCE methods.

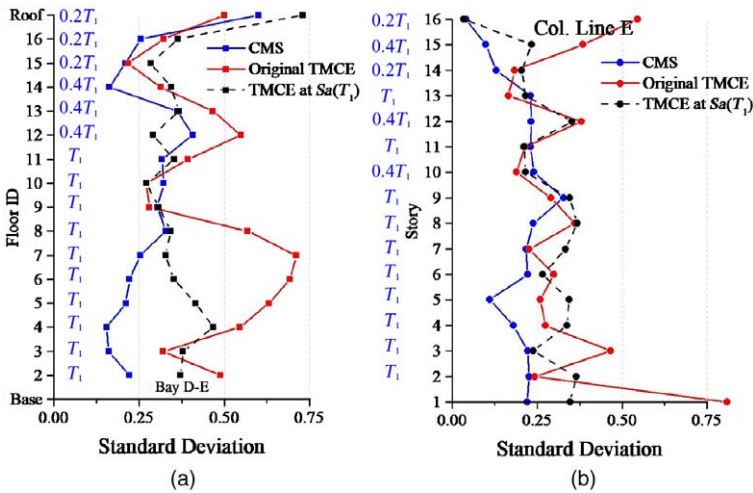


**Figure 9.** Standard deviation of the *DCR* results for the 16-story building at bay D-E of the (a) RBS connections and (b) column hinges in the column located on column line E using CMS at the controlling period and TMCE methods.

The CMS method usually leads to higher  $\sigma_{DCR,CMS}$  values for RBS connections of the 4-story frame (Figure 7), but  $\sigma_{DCR,TMCE}$  and  $\sigma_{DCR,TMCE,SaT1}$  are larger for the 8 and 16-story buildings (Figures 8 and 9). The main factor determining whether the CMS method renders the smallest dispersion is the controlling CMS period. For the 4-story beams, the

controlling period is  $0.4T_1$ , whereas most floors in the 8 and 16-story building have  $T_1$  as the controlling period. Figures 8a and 9a show that the CMS method generally leads to the smallest dispersion  $\sigma_{DCR,CMS}$  if  $T_1$  is the controlling period.

For the column hinge elements in the 4-story frame, the CMS method leads to the lowest dispersion in the 2nd and 3rd story columns, in which the controlling period is  $T_1$  (Figure 7b). Figures 8b and 9b show that the CMS GMs also lead to a lower dispersion in most columns of the 8 and 16-story frames, where the controlling period is  $T_1$ . The lower CMS dispersion is relative to that of the TMCE method and does not provide information on the accuracy of the estimated response.

Therefore, if the CMS controlling period is not  $T_1$ , the uncertainty in the response is likely to be larger for the CMS method because the spectral accelerations exhibit dispersion at  $T_1$ , and there is response variability even within the elastic system performance. Moreover, the dispersion at higher modes is also different from zero, unless the controlling period (e.g.,  $0.4T_1$ ) coincidentally corresponds to one of these higher modes. As an example, dispersion trends are shown in Figure 10 for the 8-story building, where the shaded areas enclose the maximum and minimum accelerations of the evaluated GMs for spectra anchored at  $T_1$  and  $0.2T_1$  periods. If the controlling period is  $T_1$ , the standard deviation of  $S_a$  at  $T_1$  is  $\sigma_{S_a,T_1} = 0$ , and for  $T_2 = 0.35T_1$ , the dispersion is  $\sigma_{S_a,T_2} = 0.34$ . Thus from the first two elastic modes, only  $T_2$  contributes to collapse capacity uncertainty, a contribution that in general is less significant for CMS because of its lower  $S_a(T_2)$ . However, if the controlling period is  $0.2T_1$ ,  $\sigma_{S_a,T_1} = 0.61 \neq 0$ , and  $\sigma_{S_a,T_2} = 0.41$  is also different from 0 because  $T_2 = 0.35T_1 \neq 0.2T_1$ . As observed in the gray contours of Figure 10, the dispersion rapidly increases as the period moves away from  $0.2T_1$ . Consequently, the  $S_a$  dispersion at higher modes is expected to be similar to that reported in the TMCE method, even if  $0.2T_1$  or  $0.4T_1$  are close to these modes.

The CMS dispersion would be reduced if the second and third modes are used as conditioning periods instead of predetermined values, such as  $0.2T_1$  and  $0.4T_1$ . This alternative

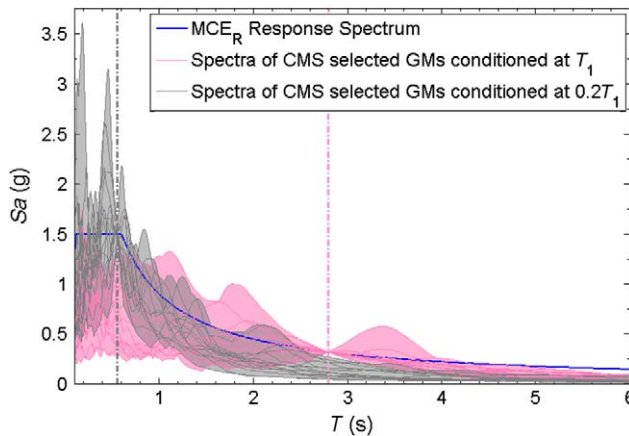


**Figure 10.** GMs selected for conditioning periods of  $T_1$  and  $0.2T_1$  for the 8-story building. The shaded area shows the bandwidth of the spectra set.

is not explored in this study, but the same criterion would apply to these conditioning periods. That is, the resulting envelope spectrum should exceed 75% maximum considered earthquake spectral accelerations in the period interval of interest.

### EFFECT OF NUMBER OF RECORDS

The premise of efficient GM selection methods is that dispersion of the response will be relatively low, and a smaller number of records can be used to estimate response parameters (Shome and Cornell 1999, Tsantaki et al. 2017). However, some  $DCR$  values exhibited large dispersion, and the 14 records used in the study may render unreliable results. Assuming a lognormal distribution, the number of records ( $n$ ) required to have an error  $X$  on the estimate of the mean, with 95% confidence, is equivalent to the following (Benjamin and Cornell 1970, Dhakal et al. 2007):

$$n = 4\sigma^2/X^2 \quad (7)$$

where  $\sigma$  is the standard deviation of the distribution. For instance, if 14 records are used, and the error in the estimate of mean  $DCR$  is within  $\pm 25\%$  (i.e.,  $X = 0.25$ , as proposed by Dhakal et al. 2007), the maximum acceptable dispersion is  $\sigma_{DCR} = 0.46$ . This practical estimate, however, may be conservative. For instance, Jalayer (2003) conducted a bootstrap procedure on 30 GMs to obtain the uncertainty in the estimation of median demand as a function of the sample size. She generated 500 bootstrap replications of subsamples  $\leq 30$  by resampling with replacement. For a standard deviation  $\sigma = 0.49$ , Jalayer (2003) determined that 12 records were needed to reduce the standard error of the estimate of median to less than 20%. For the  $X$  and  $\sigma$  values used by Jalayer, however, Equation 7 indicates that 24 records are required to have a 95% confidence on the selected mean estimate limits.

Assuming  $X = 0.25$ , Equation 7 shows that 14 records provide reliable drifts only for the  $TMCE$  at  $S_a(T_1)$  method, given that  $\sigma_{DCR,TDST1} < 0.46$  for all beam and column components. For the 8-story building, Figure 8 shows that dispersions largely exceed the  $\sigma_{DCR} = 0.46$  threshold for the CMS and  $TMCE_{SaT1}$  methods. In the case of the 16-story building (Figure 9), the CMS and  $TMCE_{SaT1}$  methods produce reliable  $DCRs$ , except for the RBS connections in the two upper stories. It is possible that a more sophisticated approach may conclude that 14 records are acceptable for some of these buildings, but that calculation is not part of the scope of this study.

### STATE OF PRACTICE: ESTIMATION OF $DCR$ MEANS USING ASCE 41 APPROACH

ASCE/SEI41 table 7-1 (ASCE 2014) indicates that the average response should be reported for a far-field site when 11 or more records are used in the analysis. This section presents  $DCR$  statistical results for the CMS and original  $TMCE$  method using the ASCE/SEI approach. The scaled-down  $TMCE$  method is not included in this section because it is not considered in ASCE/SEI 41. The arithmetic mean using all reported drifts (including 20% drift for collapsed cases) is used to compute the  $DCR$ . Thus the only acceptance criterion is  $DCR < 1.0$ .

Figure 11a shows the mean and median  $DCR$  values for the RBS hinges of the 4-story building, using the original  $TMCE$  and CMS methods. The median curves are independent of the

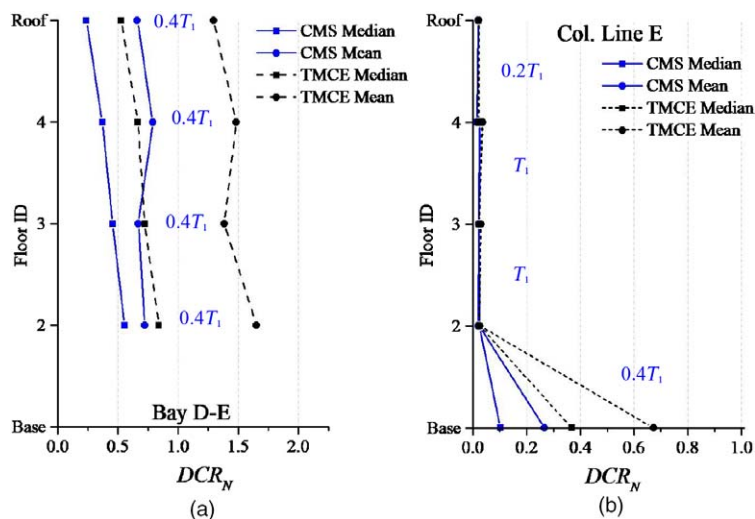


**Figure 11.** Comparison of maximum  $DCR$  mean values of the 4-story building calculated using arithmetic mean for the (a) RBSs and (b) column hinges, computed for GMs selected using the CMS and TMCE methods (the controlling CMS period of the element at each story/floor is reported in the figure).

assumed probability density function and the same for the lognormal distribution (see Figure 5a) and the ASCE/SEI 41 approach. The CMS method provides lower  $DCR$  than those obtained from the TMCE method at every floor level, with mean  $DCR_{CMS}/DCR_{TMCE}$  ratios ranging from 0.44 to 0.53. Figure 11a shows that the RBS connections do not meet the ASCE/SEI 41 acceptance criteria ( $DCR > 1.0$ ) for the TMCE method.

The large discrepancy between mean and median curves in Figure 11a is the result of using a drift of 20% to stop the analysis when computing the arithmetic mean of realizations with very large displacements. According to Table 1, seven of the nine frame-GM selection method combinations experience at least one collapse, which disproportionately increases the arithmetic mean  $DCR$ . These large differences were not observed for the lognormal sorted data approach, in which the medians and means are very similar, because the computed mean is based on the 16th and 84th percentiles (Equation 5), and it is not affected by the assumed arbitrary drifts of 20% for collapse realizations.

The  $DCR$  curves for the 4-story frame column hinges are also smaller for the CMS method, Figure 11b, with  $DCR_{CMS}/DCR_{TMCE}$  ratios varying from 0.40 to 0.93. The spectral shape and larger average spectral accelerations in the TMCE method lead to a higher level of nonlinearities and larger  $DCR$  in the components (Figure 4d). The large TMCE mean  $DCR$  at the first floor of about 0.7, Figure 11b, reflects the contribution of two collapsed realizations (Table 1).

As shown in Figure 12a, the mean  $DCR$  values for the 8-story RBS components are more than three times larger for the TMCE method than the CMS method ( $DCR_{CMS}/DCR_{TMCE} = 0.32$ ). The column hinges in the 8-story frame also provide a lower response for the CMS method, with  $DCR_{CMS}/DCR_{TMCE}$  ratios as low as 0.25 (Figure 12b). Therefore, the mean values are

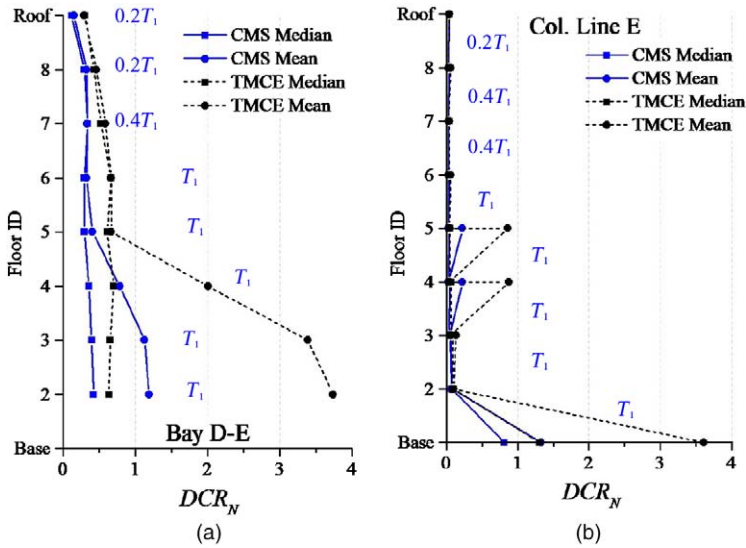


**Figure 12.** Comparison of maximum  $DCR$  mean values of the 8-story building calculated using arithmetic mean for the (a) RBSs and (b) column hinges computed for GMs selected using the CMS and TMCE methods.

significantly larger because of the presence of collapsed cases, whereas median  $DCR$  values are not affected by the collapse realizations. Figure 13 shows that the mean  $DCR$  for the 16-story building RBS and column hinge components are lower when the CMS method is used. The CMS method

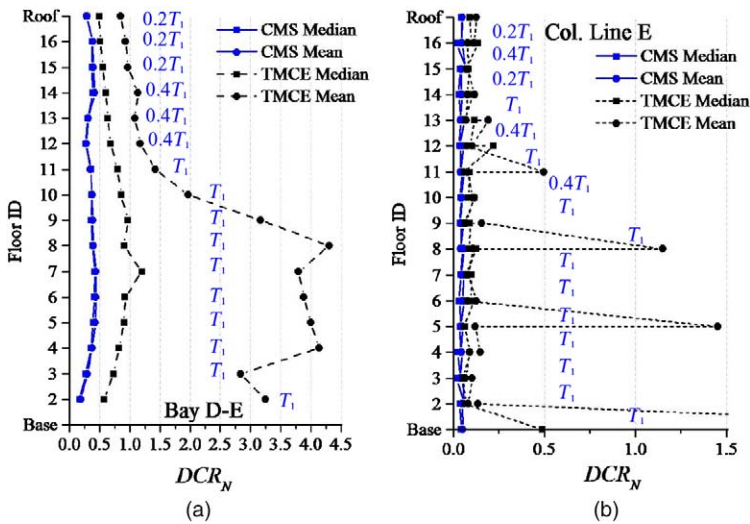


**Figure 13.** Comparison of maximum  $DCR$  mean values of the 16-story building calculated using arithmetic mean for the (a) RBSs and (b) column hinges computed for GMs selected using the CMS and TMCE methods.

meets the criteria for beams and columns (i.e.,  $DCR < 1.0$  for all components), but the original TMCE method exceeds this criterion.

Figures 11–13 show that the mean and median curves are only close to each other for the 16-story building computed with the CMS method because there are no collapse or unbounded drift realizations affecting the arithmetic mean because of an arbitrary drift (Table 1). Moreover, the inclusion of these large drifts in the realizations results in a lack of compliance in most cases.

## SUMMARY OF RESULTS

Tables 2 and 3 summarize the response of RBS components and column hinges, respectively, for the 4, 8, and 16-story frames under the three GM selection methods. The first six data columns show the maximum  $DCR$  mean ( $\mu$ ) and standard deviation of the log of the data ( $\sigma_{lnx}$ ) for both the lognormal sorted data approach and ASCE 41 methodology. For statistical values based on the sorted data, the realizations need to comply with two acceptance criteria: (1)  $DCR < 1.0$  and (2) less than 16% of collapses for the set of GMs. For results based on ASCE-41, only the first criterion is required.

For a lognormal distribution, Table 2 shows that the three buildings have  $DCR < 1.0$  for RBS components when the CMS and  $TMCE_{SaT_1}$  methods are used. For the original TMCE method, however, only the 4-story frame has acceptable maximum  $DCR$  ratios, whereas the 16-story frame has a maximum  $DCR_{TMCE} = 1.51 > 1.0$ , and the 8-story frame has four collapses (Table 1), failing the second compliance criteria. For the ASCE 41 procedure, most  $DCR$ s are  $> 1.0$  and out of compliance. According to Table 2, only three cases exhibit  $DCR$  ratios for RBS components less than unity for the ASCE-41 approach: the 4-story frame under the CMS method, and the 16-story frame under the CMS and TMCE at  $S_a(T_1)$  methods. Similar trends are observed for the column hinges in Table 3.

Regarding the maximum dispersion, Tables 2 and 3 show that the CMS method does not always lead to the smallest standard deviation. For the 4-story frame, the CMS renders the largest dispersion because the controlling period is  $0.4T_1$ . For the 8 and 16-story frames, the CMS methods provides a smaller dispersion than the TMCE methods.

The two rightmost columns of Tables 2 and 3 show the minimum and maximum mean  $DCR_{CMS}/DCR_{TMCE}$  and  $DCR_{CMS}/DCR_{TMCE,SaT_1}$  ratios for the RBS and column hinges, respectively. The mean  $DCR$  ratios are computed for every RBS or column hinge, and the maximum and minimum mean values are computed using  $DCR$ s obtained from different GM selection methods at each component. Tables 2 and 3 show that the CMS method consistently has smaller mean  $DCR$ s than those obtained from the original TMCE method (i.e.,  $DCR_{CMS}/DCR_{TMCE} < 1.0$ ). On the other hand,  $DCR_{CMS}/DCR_{TMCE,SaT_1}$  ratios are larger and the maximum ratios often exceed the unity (last column of Tables 2 and 3). Because the CMS and  $TMCE_{Sa(T_1)}$  methods have the same  $S_a$  at the conditioning period (Figure 4d), the  $DCR_{CMS}/DCR_{TMCE,SaT_1}$  ratios larger than unity indicate that the CMS lower accelerations for the rest of the spectrum are not a necessary condition to always reduce the  $DCR$ s.

**Table 2.** Maximum  $DCR$  mean and standard deviation for the three GM selection methods, and minimum and maximum mean  $DCR_{CMS}/DCR_{TMCE}$  and  $DCR_{CMS}/DCR_{TMCE,SdTI}$  ratios for RBS components

Stat. method	Building	$DCR_{CMS}$			$DCR_{TMCE}$			$DCR_{TMCE,SdTI}$			Min and max mean $DCR$	
		Max $\mu$	Max $\sigma_{lnx}$	Max $\sigma_{lnx}$	Max $\mu$	Max $\sigma_{lnx}$	Max $\sigma_{lnx}$	Max $\mu$	Max $\sigma_{lnx}$	$CMS/TMCE$	$CMS/TMCE,SdTI$	
Lognormal sorted data	4 story	0.56	0.82	0.91	0.91	0.56	0.33	0.76	0.33	0.46 and 0.68	0.58 and 0.76	
	8 story	0.46	0.77	NC-2 <sup>b</sup>	NC-2 <sup>b</sup>	NC-2 <sup>b</sup>	0.80	0.36	0.80	N/A <sup>c</sup>	0.90 and 1.76	
	16 story	0.44	0.60	1.51 <sup>a</sup>	1.51 <sup>a</sup>	0.71	0.73	0.57	0.73	0.28 and 0.72	0.60 and 1.05	
ASCE 41	4 story	0.79	N/A	1.65 <sup>a</sup>	1.65 <sup>a</sup>	N/A	N/A	1.18 <sup>a</sup>	N/A	0.44 and 0.53	0.61 and 0.80	
	8 story	1.18 <sup>a</sup>	N/A	3.74 <sup>a</sup>	3.74 <sup>a</sup>	N/A	N/A	1.25 <sup>a</sup>	N/A	0.32 and 0.71	0.82 and 1.29	
	16 story	0.44	N/A	4.31 <sup>a</sup>	4.31 <sup>a</sup>	N/A	0.67	0.67	N/A	0.057 and 0.4	0.58 and 0.95	

<sup>a</sup> Not in compliance with Acceptance Criterion 1 because  $DCR > 1.0$ .

<sup>b</sup> Not in compliance with Acceptance Criterion 2 because of more than 16% of collapsed cases.

<sup>c</sup> Not applicable.

**Table 3.** Maximum *DCR* mean and standard deviation for the three GM selection methods, and minimum and maximum mean  $DCR_{CMS}/DCR_{TMCE}$  and  $DCR_{CMS}/DCR_{TMCE,Sd(T1)}$  ratios for the column hinges

Stat. method	Building	$DCR_{CMS}$			$DCR_{TMCE}$			$DCR_{TMCE,Sd(T1)}$			Min and max mean <i>DCR</i>		
		Max $\mu$	Max $\sigma_{Inx}$	Max $\sigma_{Inx}$	Max $\mu$	Max $\sigma_{Inx}$	Max $\sigma_{Inx}$	Max $\mu$	Max $\sigma_{Inx}$	Max $\mu$	Max $\sigma_{Inx}$	$CMS/TMCE$	$CMS/TMCE,Sd(T1)$
Lognormal sorted data	4 story	0.14	0.75	0.40	0.40	0.40	0.36	0.33	0.36	0.34	1.18	0.41	1.12
	8 story	1.05 <sup>a</sup>	0.88	NC-2 <sup>b</sup>	NC-2 <sup>b</sup>	NC-2 <sup>b</sup>	1.12	1.20 <sup>a</sup>	1.12	N/A <sup>c</sup>	N/A <sup>c</sup>	0.76	1.93
	16 story	0.13	0.33	0.81	0.68	0.81	0.37	0.18	0.37	0.15	0.98	0.57	1.17
ASCE 41	4 story	0.27	N/A	N/A	0.67	N/A	N/A	0.46	N/A	0.40	0.93	0.58	1.01
	8 story	1.33 <sup>a</sup>	N/A	N/A	3.62 <sup>a</sup>	N/A	N/A	1.25 <sup>a</sup>	N/A	0.25	0.97	0.49	1.33
	16 story	0.12	N/A	N/A	3.45 <sup>a</sup>	N/A	N/A	0.19	N/A	0.027	1.6	0.24	2.39

<sup>a</sup> Not in compliance with Criterion 1:  $DCR < 1.0$ .

<sup>b</sup> Not in compliance with Criterion 2: less than 16% of collapsed cases.

<sup>c</sup> Not applicable.

## CONCLUSIONS

This study evaluates the effect of two common GM selection methods on the response of 4, 8, and 16-story steel SMFs subjected to 14 GMs using the CMS and TMCE methods. A comparison of statistical parameters for the RBSs and column hinges is conducted using the normalized  $DCR$  as output parameter. The statistical comparison considered (1) a lognormal density function and (2) the arithmetic mean, as proposed in ASCE/41-13. The main findings are as follows:

- The ASCE/SEI 41 standard does not provide a clear guidance about how to incorporate collapse realizations into the calculations. The recommendation of using the arithmetic mean to compute  $DCR$  is ambiguous for these cases because the average response is highly influenced by the selected threshold drift ratio (20% in this study), which is an arbitrary decision.
- An alternative sorted data approach is proposed to compute statistical data, assuming a lognormal distribution and the following acceptance criteria: (1)  $DCR < 1.0$  and (2) the number of collapsed cases  $< 16\%$  of the realizations. Otherwise, the structure has to be redesigned. The median of the data is the 50th of the sorted data, whereas the mean and standard deviation of the log of the data are computed with Equations 5 and 6, respectively. The implementation of this approach is straightforward and independent of the number of GMs. More importantly, the method removes the ambiguity in case of collapse because there is no need to (1) arbitrarily select a threshold collapse drift or (2) exclude collapsed realizations.
- In terms of the mean  $DCR$  ( $\mu_{DCR}$ ), the CMS method meets the two sorted data approach acceptance criteria for the 4 and 16-story frames. For the 8-story frame, the mean  $DCR$  is only slightly exceeded in the first floor ( $\mu_{DCR} = 1.05$ ).
- The current guidelines lead to a TMCE spectrum that usually has higher spectral accelerations than those of the envelope CMS spectrum. For the evaluated buildings, this results in drifts up to six times larger than those obtained from the CMS method as well as more collapse cases. The TMCE method meets the sorted data approach criteria only for the 4-story frame.
- A scaled-down mean TMCE spectrum at  $S_a(T_1)$  was also evaluated to separate the spectral shape effect on the response (Figure 4d). The  $TMCE_{SaT_1}$  spectrum leads to similar mean ( $\mu_{DCR}$ ) and standard deviation  $DCR$  ( $\sigma_{DCR}$ ) values than those from the CMS method (see Tables 2 and 3 and Figures 5 and 6). These results indicate that, for the evaluated buildings, the main difference between CMS and TMCE methods does not arise from the spectral shape adopted by each method, but from the larger spectral accelerations of the original TMCE method.
- It is assumed that the CMS controlling period is the one leading to the largest  $\mu_{DCR}$ . The  $DCR$  dispersion for this component is also associated with this conditioning period. The ASCE 41 standard does not provide guidelines in this respect.
- The  $\sigma_{DCR}$  values tend to be smaller when computed with the CMS method, and the controlling period is  $T_1$ , because there is no GM variability at  $T_1$ . The CMS method leads to lower  $DCR$  dispersion in approximately 88% of the building components in which  $T_1$  is the controlling period but only in 55% of the elements when  $T_1$  is not

the controlling period. Overall, the CMS method provides a lower dispersion 75% of the time across the results of the three buildings, regardless of the controlling period.

- To reduce the *DCR* dispersion when the CMS conditioning period is not  $T_1$ , it is proposed to assign conditioning periods to the second and third modes, instead of preselected values, such as  $0.2T_1$  and  $0.4T_1$ .
- The 14 GMs of the study as well as the ASCE/SEI minimum required number (11) may lead to unreliable results if the *DCR* dispersion is large. The assumption that an error on the mean estimate of  $\pm 25\%$  can be predicted with a 95% confidence, resulted in RBS or column hinge *DCR* dispersion that exceeds the acceptable standard deviation. Thus the number of records would need to increase for most of the cases, given the relatively large dispersions of some of the components. This verification can be easily implemented using Equation 7, but it may render conservative results. Alternatively, more advanced methods (e.g., bootstrap) can be used to show whether the results are reliable.

The study shows that the GM selection methodology and data processing decisions have a significant impact on the outcome for a set of steel SMFs within the range of 4 to 16 stories. Although the CMS method requires more effort in the selection and assessment process, it provides a GM set that is considered more realistic than that of the TMCE methods. However, the expected CMS lower drift dispersions are not always achieved, particularly when the conditioning period is not  $T_1$ . The TMCE methods resulted in even higher dispersions. The careful record selection performed in this study was not sufficient to noticeably increase the efficiency of the GMs. Thus the number of records required in the code should be increased for the current GM selection methods, or the efficiency of the GM set should be verified by means of confidence interval or bootstrap methods.

### ACKNOWLEDGMENTS

The authors are grateful to the three independent reviewers who greatly improved the clarity and quality of this paper. The authors also appreciate the fruitful discussions with Fatemeh Jalayer during the preparation of the manuscript.

### REFERENCES

- Adam, C., Kampenhuber, D., Ibarra, L. F., and Tsantaki, S., 2016. Optimal spectral acceleration-based intensity measure for seismic collapse assessment of P-delta vulnerable frame structures, *Journal of Earthquake Engineering* **21**, 1189–1195.
- American Institute of Steel Construction, 2010. *Seismic Provisions for Structural Steel Buildings, ANSI/AISC 341-10*, Chicago, IL.
- American Society of Civil Engineers (ASCE), 2010. *Minimum Design Loads for Buildings and Other Structures, ASCE/SEI 7-10*, Reston, VA.
- American Society of Civil Engineers (ASCE), 2014. *Seismic Evaluation and Retrofit of Existing Buildings, ASCE/SEI41-13*, Reston, VA.
- American Society of Civil Engineers (ASCE), 2016. *Minimum Design Loads for Buildings and Other Structures, ASCE/SEI 7-16*, Reston, VA.
- Baker, J. W., 2011. Conditional mean spectrum: Tool for ground motion selection, *Journal of Structural Engineering* **137**, 322–331.

- Baker, J. W., 2016. Software for selecting earthquake ground motions to match a target conditional spectrum, available at [http://web.stanford.edu/~bakerjw/gm\\_selection.html](http://web.stanford.edu/~bakerjw/gm_selection.html) (last accessed 9 September 2016).
- Benjamin, J. R., and Cornell, C. A., 1970. *Probability, Statistics, and Decisions for Civil Engineers*, McGraw-Hill, New York, NY, 684 pp.
- Bradley, B. A., 2010. A generalized conditional intensity measure approach and holistic ground-motion selection, *Earthquake Engineering Structural Dynamics* **39**, 1321–1342.
- Campbell, K. W., and Bozorgnia, Y., 2008. NGA ground motion model for the geometric mean horizontal component of PGA, PGV, PGD and 5% damped linear elastic response spectra for periods ranging from 0.01 to 10 s, *Earthquake Spectra* **24**, 139–171.
- Computers and Structures, Inc., 2011. *PERFORM-3D*, Berkeley, CA, available at <https://www.csiamerica.com/products/perform-3d>.
- Dhakal, R. P., Singh, S., and Mander, J. B., 2007. Effectiveness of earthquake selection and scaling method in New Zealand, *Bulletin of the New Zealand Society for Earthquake Engineering* **40**, 160–161.
- Harris, J. L., III, and Speicher, M. S., 2015. *Assessment of First Generation Performance-Based Seismic Design Methods for New Steel Buildings, Volume 1: Special Moment Frames*, NIST Tech. Note 1863-1, National Institute of Standards and Technology, Gaithersburg, MD.
- Haselton, C. B., Baker, J. W., Bozorgnia, Y., Goulet, C. A., Kalkan, E., Luco, N., Shantz, T. J., Shome, N., Stewart, J. P., Tothong, P., Watson-Lamprey, J. A., and Zareian, F., 2009. *Evaluation of Ground Motion Selection and Modification Methods: Predicting Median Intersitory Drift Response of Buildings*, PEER Report 2009/01, Pacific Earthquake Engineering Research Center, Berkeley, CA.
- Ibarra, L., and Krawinkler, H., 2005a. Effect of uncertainty in system deterioration parameters on the variance of collapse capacity, Paper 107, in *Proceedings, Ninth International Conference on Structural Safety and Reliability*, June 19–23, 2005, Rome, Italy.
- Ibarra, L. F., and Krawinkler, H., 2005b. *Global Collapse of Frame Structures under Seismic Excitations, Rep. No. 152*, Pacific Earthquake Engineering Research Center, Berkeley, CA.
- International Code Council, 2012. *2012 International Building Code*. Washington, DC.
- Jalayer, F., 2003. Direct Probabilistic Seismic Analysis: Implementing Non-linear Dynamic Assessments, Ph.D. Dissertation, Stanford University, Stanford, CA.
- Jayaram, N., Lin, T., and Baker, J. W., 2011. A computationally efficient ground-motion selection algorithm for matching a target response spectrum mean and variance, *Earthquake Spectra* **27**, 797–815.
- Kalkan, E., and Chopra, A. K., 2010. *Practical Guidelines to Select and Scale Earthquake Records for Nonlinear Response History Analysis of Structures*, U.S. Geological Survey Open-File Report 2010, Reston, VA.
- Kohrangi, M., Bazurro, P., Vamvatsikos, D., and Spillatura, A., 2017. Conditional spectrum-based ground motion record selection using average spectral acceleration, *Earthquake Engineering & Structural Dynamics* **46**, 1667–1685.
- Krawinkler, H., 1978. Shear in beam-column joints in seismic design of steel frames, *Engineering Journal* **15**, 82–91.
- Krawinkler, H., Zareian, F., Medina, R. A., and Ibarra, L., 2004. Contrasting performance-based design with performance assessment, in *Performance-Based Seismic Design Concepts and*

- Implementation: Proceedings of an International Workshop* (P. Fajfar and H. Krawinkler, eds.), Pacific Earthquake Engineering Research Center, Berkeley, CA, 505–516.
- Lin, T., Haselton, C. B., and Baker, J. W., 2013. Conditional spectrum-based ground motion selection. Part I: Hazard consistency for risk-based assessments, *Earthquake Engineering & Structural Dynamics* **42**, 1847–1865.
- Miano, A., Jalayer, F., Ebrahimian, H., and Prota, A., 2018. Cloud to IDA: Efficient fragility assessment with limited scaling, *Earthquake Engineering & Structural Dynamics* **47**, 1124–1147.
- National Institute of Standards and Technology, 2011. *Selecting and Scaling Earthquake Ground Motions for Performing Response History Analyses*, NIST GCR 11-917-15, Gaithersburg, MD.
- Pacific Earthquake Engineering Research Center (PEER), 2016. PEER Ground Motion Database, available at <http://ngawest2.berkeley.edu/> (last accessed 9 September 2016).
- Sattar, S., Liel, A. B., and Martinelli, P., 2013. Quantification of modeling uncertainties based on the blind prediction contest submissions, in *Proceedings, Structures Congress 2013* (B. J. Leshko and J. McHugh, eds.), ASCE, Reston, VA, 1997–2008.
- Shome, N., and Cornell, C. A., 1999. *Structures*, UMI, Ann Arbor, MI.
- Tsantaki, S., Adam, C., and Ibarra, L. F., 2017. Intensity measures that reduce collapse capacity dispersion of P-delta vulnerable simple systems, *Bulletin of Earthquake Engineering* **15**, 1085–1109.
- Uribe, R., Sattar, S., Speicher, M. S., and Ibarra, L., 2017. Influence of ground motion selection on the assessment of steel special moment frames, Paper No. 2410, in *Proceedings, 16<sup>th</sup> World Conference on Earthquake*, 9–13 January 2017, Santiago, Chile.
- Uribe, R., Sattar, S., Speicher, M. S., and Ibarra, L., 2018. *Impact of Ground Motion Selection Methods on the Seismic Assessment of Steel Special Moment Frames*, NIST TN-1992, National Institute of Standards and Technology, Gaithersburg, MD.
- U.S. Geological Survey (USGS), 2016. Custom Vs30 mapping, available at <http://earthquake.usgs.gov/hazards/apps/vs30/custom.php> (last accessed 9 September 2016).

(Received 29 December 2017; Accepted 19 February 2019)